Electronic Supplementary Material (ESI) for Physical Chemistry Chemical Physics

Electronic Supplementary Information

Electron transfer with azurin at Au/SAM junctions in contact with a protic ionic melt: Impact of glassy dynamics

Dimitri E. Khoshtariya*[a,b,c,d], Tina D. Dolidze[a,b,c], Tatyana Tretyakova[a,b], David H. Waldeck[d,1] and Rudi van Eldik*[a]

[a]*Department of Chemistry and Pharmacy, University of Erlangen-Nürnberg, 91058 Erlangen, Germany, E-mail: vaneldik@chemie.uni-erlangen.de*

[b]*Institute for Biophysics and Bio-Nanosciences, Department of Physics, Tbilisi State University, 0128 Tbilisi, Georgia. E-mail: dimitri.khoshtariya@tsu.ge*

[c]*Department of Biophysics, Center for Experimental Biomedicine, 0160 Tbilisi, Georgia*

[d]*Department of Chemistry, University of Pittsburgh, Pittsburgh, PA 5260, USA. E-mail: dave@pitt.edu*

High-Pressure Unit and Electrode Handling

These issues were described in earlier work, Refs. S1-S4. In brief, the working electrode was a 1.6 mm diameter gold disc sealed in a Teflon cylinder (BAS) and it was sealed into the cell cap by two O-rings, together with the auxiliary electrode (platinum wire) and the quasi-reference electrode - silver wire. Throughout these experiments the latter has not been placed in a plastic tube (with a Vycor tip at the end) as reported previously,[S1-S4] due to the technical difficulties of handling the high-pressure cell while filling by semi-solid working solutions. Importantly, knowledge of the formal (midpoint) potential, E_o (versus the standard electrode) for immobilized redox species (Az) are not required for the extraction of kinetic parameters in the framework of a Marcus model, through the CV data analysis.[S10-S12] An impact of choline dihydrogen phosphate ([ch][dhp]) additives on E_o will be thoroughly studied in a separate work. The home-made high-pressure electrochemical cell was filled by the PIM at high temperature, typically 50 to 70 ^{o}C, at which any PIM was liquid-like, and electrochemical measurments were started from this point. The assembled pressure vessel, which contained the electrochemical cell, was placed into a special a thermostatted water jacket integrated into the high-pressure vessel. The temperature was controlled within ± 0.1 ^{o}C using a digital temperature controller.

All the gold working electrodes were coated by a self-assembled monolayer and the protein by the standard protocol. First the gold disc was sequentially polished with a 0.5 μm and then a 0.05 μm alumina water slurry, then it was washed with deionized water, and finally it was treated in an ultrasonic bath for 3 min. Next the bare gold electrodes were electrochemically cleaned by cycling them between –0.35 and 1.4 V (versus Ag/AgCl/3M NaCl) in a 0.5 M H_2SO_4 solution at a scan rate 0.1 V s^{-1} for at least 1 hour (until reproducible voltammograms for clean gold were recorded). Following this procedure, the electrodes were rinsed with ultrapure water and ethanol. Self-assembled monolayers were prepared by direct immersion of freshly cleaned electrodes in ethanol solutions of the corresponding 5×10^{-3} M alkanethiols for 24 hours.[S4] Before the protein immobilization, the SAM modified electrodes were thoroughly rinsed with ethanol,

then water, and finally with a buffer solution. The SAM coated electrodes were then transferred into a 140 μM Az solution with 5 mM NH_4Ac added (pH 4.6) for up to 2 min.[S5] It was found that even a few tens of seconds of rinsing was sufficient to obtain properly arranged films of Az resulting in a nearly ideal voltammetric response; see Figure 1 (main body).

Measurements and Data Processing

The solution resistance R_S between the surface of the working electrode and the tip of the reference electrode was calculated using Eq. S1[S6]

$$R_S = \arctan(r_r / r_w) / (2\pi\, r_w\, \kappa) \qquad \text{(S1)}$$

where r_w is the radius of the working electrode, κ is the conductivity of the medium and r_r is the distance between the working and reference electrodes, which in our high-pressure cell had to be positioned 1.0 cm from the working electrode. The values of R_S at different temperatures were calculated by taking into account changes in conductivity of the solution with temperature and pressure.[S4] The average change (lowering) of the k^o value, which arose from the Ohmic potential drop before the applied correction, was typically only about 2 %, while in exceptional cases the correction was about 10 %. Note that the error arising from overly high values of R_s (the lack of the IR_S correction) is apparent from the fitting procedure because it results in an increasing deviation of experimental points from the theoretical curve. This discrepancy disappears upon the proper IR_S correction.[S4]

The surface coverage of electrochemically active Az (Γ) was determined in each case by considering the voltammogram's peak areas (θ), through Eq. S2[S5]

$$\Gamma = \theta / (n\, F\, S\, v) \qquad \text{(S2)}$$

where n is the number of transferred electrons taken as 1, F is the Faraday constant, S is the geometric area of the electrode, and v is the potential scan rate. The surface coverage for the 1-pentanethiol and 1-hexadecanethiol SAM modified gold electrodes was determined at ambient pressure and 2 ^oC and fluctuated from sample to sample with an average between 4 and 17 pmol

cm^{-2}.[S7,S8] In the previous work,[S4] a very slow decrease in peak height was observed during measurements, and a drastic surface coverage decrease occurred at temperatures above 45 ^{o}C and in the course of pressure release at any pressure level above 5 MPa. In contrast, the Au/SAM/Az, assemblies in contact with [ch][dhp] electrolyte, especially, for melts with lower water content, viz., the W/IP ratio of ≤ 3.7, did not show such effects, and the CV signal was even found to be stable over multiple cycling during several days throughout the temperature or/and pressure cycling within 0 to 80 ^{o}C and 0 to 150 MPa, respectively. Above 80 ^{o}C a considerable decrease of the signal intensity, presumably caused by Az detachment, was detected.

Results and Discussion (Additional Details)

The voltammetric studies of Au/SAM/Az, assemblies under variable experimental conditions ([ch][dhp] concentration, *T* and *P*), in most cases, were undertaken repeatedly (normally, 2 to 3 times) unless their reliability was determined not to be satisfactory. For the particular cases of 50 and 70 % PIM blends, in which the kinetic results were taken to lie in the non-ergodic zone (exhibiting irregular and irreproducible behavior; Fig. 6*A* and *B*), the temperature studies were reproduced for seven different samples and fourteen repetitive scans, and the pressure studies used two different samples and four repetitive scans, for the better corroboration of the anomalous pattern. Kinetic data on *P* dependencies for 80 and 85 % PIM blends taken at 50 ^{o}C, which are presented in Fig. 5, were collected for a single sample for each blend because of the unique character of the respective experimental conditions. Specifically, at *T* = 323 K (50 ^{o}C) lengthy annealing periods were used in order to achieve better thermal equilibration of the systems' inherent relaxation modes throughout the pressure cycling protocol. Nevertheless, the results depicted in Fig. 5 should be considered as highly reliable for the following reasons: (a) the starting and final measurements within the *P* cycling yielded virtually the same kinetic results for both of these blends, despite the fact that the second blend exhibited a strong anomaly

at higher *P*; (b) kinetic data displayed very similar patterns of near independence of the rate constant on *P* upon the pressure rise; (c) for each of these two samples, at seven different pressure levels, in total at least ten independent measurements of k^o were performed (each measurement implying CV recording at least at 10 to 20 potential sweep rates). Hence, all the results should be considered as free of any serious artifacts.

Fig. 2*A* and *B* show representative fitting curves accomplished for distinct experimental series, in which cases a procedure based on the Marcus model was used.[S10-S12] Note that $\Delta E = E_{peak} - E_o$, where E_{peak} is the peak potential and E_o is the formal redox (peak midpoint) potential under the given experimental conditions, was plotted versus the potential scan rate divided by the unimolecular standard rate constant. All the experimental CV curves were symmetrical with respect to the anodic and cathodic peak height and shape (Fig. 1*A* and *B*). Figures 3*A* and *B* demonstrate analogous fitting curves for CV data obtained for cases where the same procedure either worked (the 85 and 90 % [ch][dhp] blends, at low pressure/high temperature), or failed to do so (the 85 and 90 % PIM blends, at high pressure/high temperature and around room temperature and lower temperatures combined with low pressure). Note that any distortions of the data by an effect of non-compensated resistance should be excluded, because it was measured and found to either be negligible or small under the experimental conditions; nevertheless the correction was applied (see above) and it does not change the conclusions.

The accuracy of this methodology is much higher for the determination of k^o (normally 5 to 15 %) than for λ_o (normally 15 to 30 %) [see, e.g. Refs. S10-S12], because the latter parameter is much more demanding regarding the statistical “capacity” of the data being processed (accuracy, number of points, etc.). Because of the global fitting procedure the accuracy for λ_o (as demonstrated in Ref. S4, it has a common value of 0.3 eV throughout all the series, see below) should be improved over that obtained by an independent analysis of each assembly type.

Fig. S2*A* shows the evolution of the conductivity for the buffered aqueous [ch][dhp] blends (pH 4.6) as a function of the mole fraction of the [ch][dhp] component, at 20 ^{o}C. Data for the pure [ch][dhp] are taken from Ref. S13. Remarkably, this dependence in its shape is very similar to one published in Ref. S14 (Fig. 5) for a typical binary water/PIL mixture. Fig. S2*B* depicts an Arrhenius-type plot for the conductivity temperature dependence of a 90% (w/w) buffered aqueous [ch][dhp] blend (pH 4.6), with both polynomial and linear fits. The linear Arrhenius fit can be considered as a restricted approximation to a more general nonlinear dependence; e.g. the Vogel-Fulcher or Vogel-Tammann-Fulcher equations (See, e.g., Refs. S15,S16). Fig. S3*A*. depicts linear (matching color) and polynomial (black dashed curves) fits of the same experimental data that are presented in Fig. 4 (see main body), with added (hypothetical) extrapolations to the higher temperature range (up to 400 K). These extrapolations are based on distinct mathematical procedures only and imply an imaginary stability of functionalized Az assemblies above 353 K. Because, seemingly, the friction controlled regime for this system is operative by a direct control of the rate constant through ν_{eff} ($1/\tau_{eff}$), Eqs. 3 to 5, i.e., by collectively reorganizable mode(s) and, to some extent, also contributing to λ_{eff} (see discussion in the main body), since such mode(s) like the abovementioned conductivity power, should follow the Vogel-Fulcher or Vogel-Tammann-Fulcher equations, see, e.g. Refs. S15,S16, the Arrhenius plots for k^0 should also be curved rather than linear. The apparent intersection of linear plots (depicted by a green arrow) at ca. 377 K is thus nonphysical. However, the actual (resulting) Arrhenius dependencies are of hybrid nature, combining the features of two contributing motifs, the essentially nonlinear one (related to ν_{eff}) and the quasi-linear one (partially contributing to the exponential term via λ_{eff}). Depicted polynomial fittings, although are solely illustrative, in fact, support this statement. Furthermore, Fig. S3*B* depicts the extrapolated double logarithmic dependence for the viscosity versus the percent w/w composition of buffered aqueous [ch][dhp] blends that were used for a rough tentative estimation of the viscosity values of higher blends and pure solid [ch][dhp] (see Table 1 for the

numerical data., all given for 20 ^{o}C). The points within red circles correspond to the literature (beforehand estimated) values for 0 (≈ 1 cp), 70 and 80 % w/w (Ref. S17) solutions, respectively.

References:

S1. T.D. Dolidze *et al*., *J. Phys. Chem. B*, 2003, 107, 7172-7179.
S2. D.E. Khoshtariya *et al*., *Chem. Eur. J.*, 2006, 12, 7041-7056.
S3. T.D. Dolidze *et al*., *J. Phys. Chem. B*, 2008, 112, 3085-3100.
S4. D.E. Khoshtariya *et al*., *Proc. Natl. Acad..Sci. USA*, 2010, 107, 2757-2762.
S5. B.D. Fleming, S. Praporski, A.M. Bond and L.L. Martin, *Langmuir*, 2008, 24, 323-327.
S6. A.M. Bond, K.B. Oldham and G.A. Snook, *Anal. Chem.*, 2000, 72, 3492-3496.
S7. Q. Chi, J. Zhang, J.E.T. Andersen and J. Ulstrup, *J. Phys. Chem. B*, 2001, 105, 4669-4679.
S8. Y. Guo, J. Zhao, X. Yin, X. Gao and Y. Tian, *J. Phys. Chem. C*, 2008, 112, 6013-6021.
S9. L.J.C. Jeuken, J.P. McEvoy and F.A. Armstrong, *J. Phys. Chem. B*, 2002, 106, 2304-2313.
S10. K. Weber, and S.E. Creager, *Anal. Chem.*, 1994, 66, 3164-3172.
S11. L. Tender, M.T. Carter and R.W. Murrey, *Anal. Chem.*, 1994, 66, 3173-3181.
S12. K. Weber, L. Hockett and S. Creager, *J. Phys. Chem. B*, 101, 8286-8291.
S13. U.A. Rana *et al*., *Phys. Chem. Chem. Phys.*, 2010, 12, 11291-11298.
S14. C. Brigouleix *et al*., *J. Phys. Chem. B*, 2010, 114, 1757-1766.
S15. C.A. Angell, *Science (Washington)*, 1995, 267, 1924-1935.
S16. T. Bauer *et al., J. Chem. Phys. B*, 2010, 133, 144509.
S17. K. Fujita and H. Ohno, *Biopolymers*, 2010, 93, 1093-1099.
S18. C**.** La Rosa *et al., J. Phys. Chem.*, 1995, 99, 14864-14870.

Table S1 A. Conductivity of [ch][dhp] blends (w/w) versus their composition, 20 ^{o}C; see also Table 1 in the main body. **B.** Conductivity of the 90% (w/w) [ch][dhp] blend vs temperature.

[ch][dhp], t = 20 °C, pH 4.6	
% (w/w)	**Conductivity, S/m**
0	**0.518**
30	**2.780**
50	**2.258**
70	**0.915**
80	**0.340**
85	**0.144**
90	**0.026**
100	**~ 0.00001 (Ref. S13)**

90% [ch][dhp] (w/w), pH 4.6	
Temperature, K	**Conductivity, S/m**
293	**0.0270**
303	**0.0424**
313	**0.0602**
323	**0.0815**
333	**0.1056**
343	**0.1430**
353	**0.1710**

Figure Legends:

Scheme S1. Molecular structure of choline dihydrogen phosphate ([ch][dhp]).

Figure S1 A. Arrhenius plots for electron transfer rate constants of Az immobilized at n-Hexadecanethiol (*n* = 15) SAM coated Au electrodes in 70 % w/w mixture of [ch][dhp] and the buffered aqueous solution, pH 4.6 (green). The Arrhenius dependence for a reference system with no [ch][dhp] additives (black) (Ref. S4) is also depicted for comparison. **B.** Pressure dependencies for ET rate constants of Az immobilized at n-Hexadecanethiol (*n* = 15) SAM coated Au electrodes in 70 % w/w mixture of [ch][dhp] and the buffered aqueous solution, pH 4.6 (green). Open and filled symbols indicate cycles with the pressure increase and decrease, respectively. The Pressure dependence for a reference system with no [ch][dhp] additives (black) (Ref. S4) is also depicted for comparison (no reverse cycle was possible in that case).

Figure S2 A. Evolution of the conductivity for the buffered aqueous [ch][dhp] blends (pH 4.6) as a function of the molar fraction of the [ch][dhp] component, at 20 ^{o}C. Data for a pure solid [ch][dhp] are taken from Ref. 31 (see also Table S1). **B.** Arrhenius-type plot for the conductivity temperature dependence of a 90% (w/w) buffered aqueous [ch][dhp] blend (pH 4.6). Blue curve – the polynomial fit; dashed red line – the linear fit.

Figure S3 A. Linear (matching color) and polynomial (black dashed curves) fits of the same experimental data that are presented in Fig. 1 (main body), with added (hypothetical) extrapolations to the higher temperature range (up to 400 K). These extrapolations are based on distinct mathematical procedures only and imply an imaginary stability of functionalized Az assemblies above 353 K. The actual (resulting) Arrhenius dependencies are of hybrid nature, combining the features of two contributing motifs, the essentially nonlinear one (related to ν_{eff}) and the quasi-linear one (partially contributing to the exponential term via λ_{eff}). Thus, the apparent intersection of linear plots (depicted by a green arrow) at ca. 377 K is nonphysical. Depicted polynomial fittings, although are solely illustrative, in fact, support this statement. **B.** The extrapolated double logarithmic dependence for the viscosity versus the % w/w composition of buffered aqueous [ch][dhp] blends, used for a rough tentative estimation for the viscosity values of higher blends and pure solid [ch][dhp] (all at ca. 20 ^{o}C). The points within red circles correspond to the literature (beforehand estimated) values for 0 (≈ 1 cp), 70 and 80 % [ch][dhp] w/w (Ref. S17) solutions, respectively, see Table 1 for the numerical data.

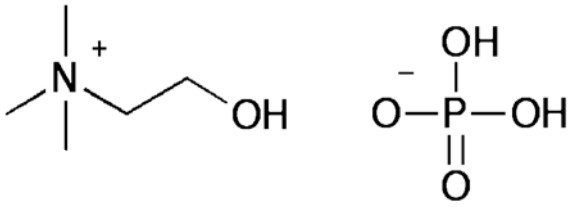

Scheme S1

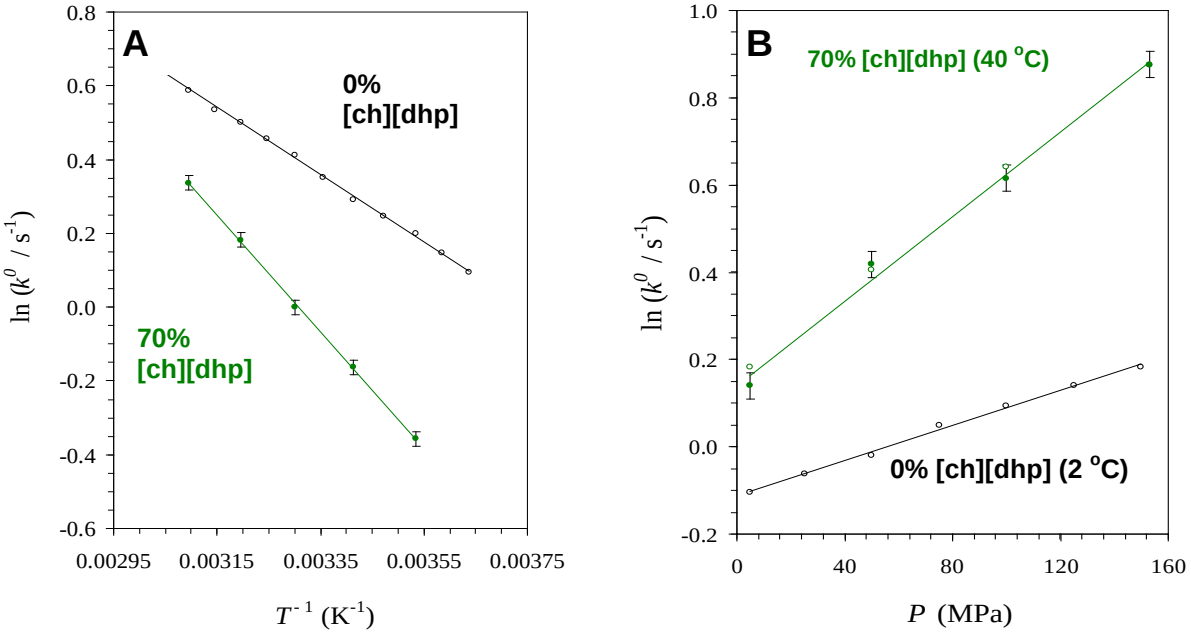

Figure S1.

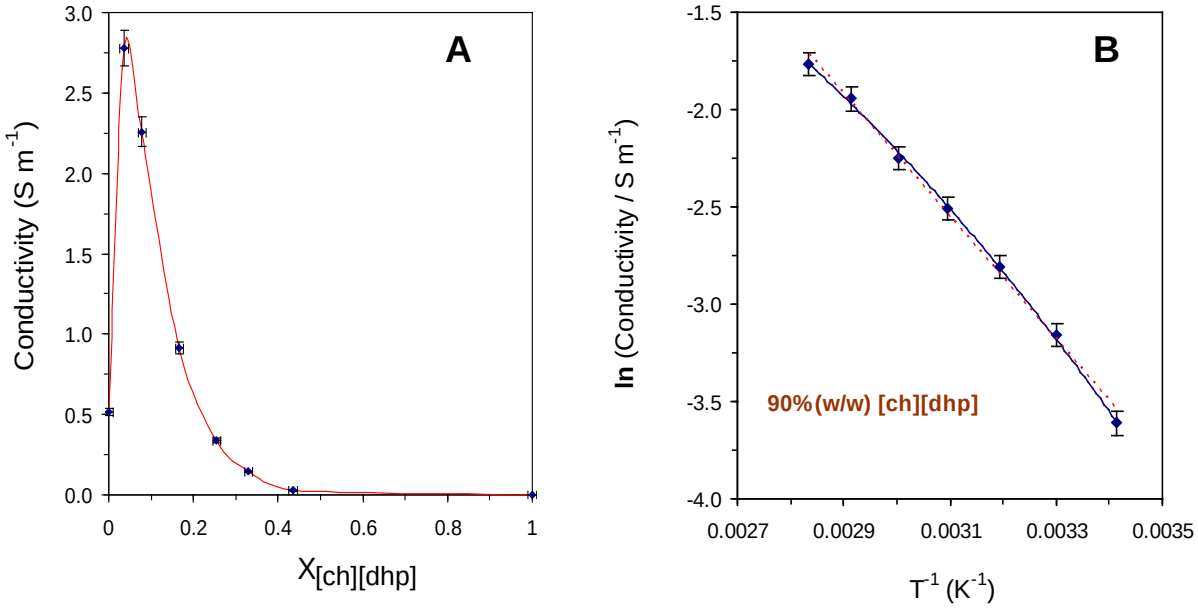

Figure S2.

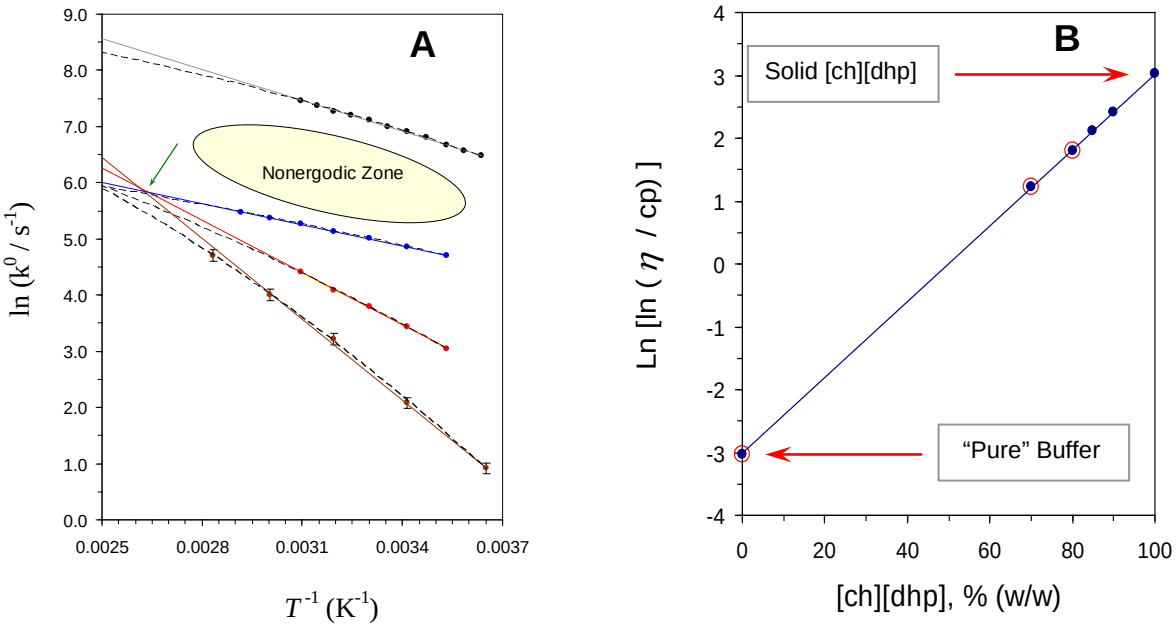

Figire S3.